Int. J. Heat Mass Transfer. Vol. 31, No. 7, pp. 1385–1398, 1988
Printed in Great Britain

0017–9310/88 $3.00 + 0.00

Non-parallel wave instability of mixed convection flow on inclined flat plates

S. L. LEE,† T. S. CHEN and B. F. ARMALY
Department of Mechanical and Aerospace Engineering, University of Missouri–Rolla, Rolla, MO 65401, U.S.A.

(*Received* 18 *May* 1987 *and in final form* 18 *November* 1987)

Abstract—A non-parallel flow analysis by an order-of-magnitude approach is performed to investigate the linear wave instability of mixed convection flow along an isothermal inclined flat plate. This analysis removes the previous restriction on the weak dependence of the streamwise variation of disturbance quantities. The resulting non-homogeneous, coupled equations for the momentum and temperature disturbances are solved by a superposition technique along with a modified Thomas transformation method. Critical Reynolds numbers are presented for inclination angles in the range of $0^\circ \leqslant \gamma \leqslant 90^\circ$ (with γ being measured from the horizontal), covering the buoyancy parameter range of $-0.15 \leqslant Gr_x/Re_x^2 \leqslant 1$ for Prandtl numbers of 0.7 and 7. It is found that the net effect of buoyancy force on the critical Reynolds number is essentially zero at $\gamma = 1.05^\circ$ when the plate is almost horizontal. For $\gamma > 1.05^\circ$, an increase in the value of Gr_x/Re_x^2 stabilizes the flow. This behavior is reversed for $\gamma < 1.05^\circ$.

INTRODUCTION

EFFORTS to clarify and to explain the process of transition from laminar to turbulent flow regime have been undertaken for many decades. Many of the studies in wave instability superpose small disturbances on the laminar mainflow to see if the disturbances decay or amplify as they travel in the streamwise direction. The objective is to predict the value of the critical Reynolds number for a prescribed laminar mainflow. The critical Reynolds number result, however, strongly depends on the characteristics of the wave form assumed for the disturbances. One of the wave forms, known as the parallel flow model, assumes that the amplitude function of the disturbance $\tilde{\Phi}$ is independent of the streamwise coordinate X (that is, $\tilde{\Phi}_x = \partial\tilde{\Phi}/\partial X = 0$). The disturbance equation thus reduces to the standard Orr–Sommerfeld equation. As applied to the Blasius flow over a flat plate, the parallel flow model predicts a critical Reynolds number of $\lambda^* = (Re_x^{1/2})^* = 302$ which is 37% higher than the experimental data ($\lambda^* = 220$) of Schubauer and Skramstad [1] and Ross *et al.* [2]. Mucoglu and Chen [3] took the effect of the mainflow transverse velocity V (the V-effect) into account in the parallel flow model, and obtained $\lambda^* = 290$ which is still much higher than the experimental data. Their model will be referred to as the 'quasi-parallel flow model' in this paper.

To remedy the discrepancy between the results by the parallel flow model and the experimental data, non-parallel flow models considering the streamwise variation of $\tilde{\Phi}$ have been proposed. In the non-parallel flow models, due to the dependence of $\tilde{\Phi}$ on X, the definition of the disturbance amplification rate depends on the growth of a certain physical quantity, such as the stream function, velocity or intensity of the disturbances. By assuming a weak X-dependence of $\tilde{\Phi}$, Bouthier [4] proposed the method of multiple scales to analyze the non-parallel linear instability of Blasius flow. The amplification rate of the disturbance then was defined by using the growth rate of disturbance kinetic energy (the same as intensity). The critical Reynolds number, however, was found to depend on the normalization of the dimensionless eigenfunction Φ_x. To fit the experimental data of $\lambda^* = 220$ (Schubauer and Skramstad [1], Ross *et al.* [2]), Bouthier chose a certain normalization to yield $\lambda^* = 205$. Based on this particular normalization, he found that the growth rate of the disturbances is two-dimensional and reaches its maximum value at the wall; that is, the least stable point occurs at the wall. This is incredible, because the wall region should be unconditionally stable due to the existence of a laminar sublayer adjacent to the wall. Later, Gaster [5] solved the same problem by using a similarity coordinate and normalized the eigenfunction Φ_x by some means. He obtained a critical Reynolds number of $\lambda^* = 271$ based on the total kinetic energy of the disturbances. Saric and Nayfeh [6] later extended the work of Bouthier [4] by considering also the V-effect. However, in defining the neutral stability curve, they did not consider the effect of the X-dependence of the disturbance intensity. Their model is thus incomplete. Very recently, ref. [7] presented a non-parallel flow analysis based on the order-of-magnitude approach so that there is no need to restrict the analysis to a weak dependence of $\tilde{\Phi}$ on X, as was done in previous

† Present address: Department of Power Mechanical Engineering, National Tsing-Hua University, Hsinchu, Taiwan 30043, R.O.C.

NOMENCLATURE

c_p specific heat at constant pressure [J kg^{-1} K^{-1}]
E amplitude function of the disturbance intensity
e $\Phi_x''(x, 0)/\Phi_0''(x, 0)$
g gravitational acceleration, 9.81 m s^{-2}
Gr_x Grashof number based on X, $\beta g(T_w - T_\infty)X^3/\nu^2$
Gr_δ Grashof number based on δ, $\beta g|T_c|\delta^3/\nu^2$
I dimensionless disturbance intensity, $(|\tilde{U}|^2 + |\tilde{V}|^2)^{1/2}/U_c$
k thermal conductivity [W m^{-1} K^{-1}]
Pr Prandtl number, ν/α
Re_x Reynolds number based on X, $U_\infty X/\nu$
Re_δ Reynolds number based on δ, $U_c\delta/\nu$
S dimensionless amplitude function of disturbance temperature, $\tilde{S}/T_c$
s normalized amplitude function of disturbance temperature, $S/\Phi_0''(x, 0)$
T temperature [K]
t time [s]
U streamwise velocity [m s^{-1}]
u dimensionless streamwise velocity, U/U_c
V transverse velocity [m s^{-1}]
v dimensionless transverse velocity, $(X/\delta)V/U_c$
X streamwise coordinate [m]
x dimensionless streamwise coordinate, X/X_c
X_0 location where the disturbance is given [m]
Y transverse coordinate [m]
y dimensionless transverse coordinate, Y/δ
y_c location in y-coordinate where β reaches its maximum value, $\beta(y_c) = \beta_{max}$.

Greek symbols
α dimensionless wave number of the disturbance, $\tilde{\alpha}\delta$; or thermal diffusivity [m^2 s^{-1}]
β stability function defined in equation (27b); or volumetric coefficient of thermal expansion [K^{-1}]
γ inclination angle of the plate measured from horizontal position [deg]
δ characteristic boundary layer thickness [m]
ε δ/X_c
ζ $\pm Gr_\delta/Re_\delta$
θ dimensionless temperature, $(T - T_\infty)/T_c$
λ Re_δ
ν kinematic viscosity [m^2 s^{-1}]
ξ local non-similarity parameter in the mainflow
ρ density [kg m^{-3}]
Φ dimensionless amplitude function of the disturbance, $\tilde{\Phi}/\delta U_c$
ϕ normalized amplitude function of the disturbance, $\Phi/\Phi_0''(x, 0)$
$\tilde{\Psi}$ stream function of the disturbance [m^2 s^{-1}]
ω dimensionless wave frequency, $\tilde{\omega}\delta/U_c$.

Superscripts
~ disturbance quantity
* properties at the critical point.

Subscripts
c characteristic quantity
i imaginary part of a complex number
nh 'nonhomogeneous'
r real part of a complex number
w condition at wall
0 quantities based on quasi-parallel flow model
1 correction to the quasi-parallel flow model
∞ condition in free stream.

investigations. A superposition technique along with a finite difference method [8] was used to solve the resulting non-homogeneous disturbance equations without recourse to the use of an adjoint eigenfunction. Reference [7] found that the normalization of the eigenfunction Φ_x is not entirely arbitrary because the condition $\Phi_x''(x, 0) = \partial\Phi_0''(x, 0)/\partial x$ gives a constraint to the value of $\Phi_x''(x, 0)$. The value of $e = \Phi_x''(x, 0)/\Phi_0''(x, 0)$, was thus treated as an arbitrary real function of x such that the neutral stability curve based on the disturbance intensity can be uniquely defined. The analysis leads to a critical Reynolds number of $\lambda^* = 217.4$ which agrees very well with the experimental data ($\lambda^* = 220$). Reference [7] also showed that the amplification rate of the disturbance intensity is two-dimensional, with a maximum occurring near the location $\eta = (Y/X)Re_x^{1/2} = 3$, and that the wall region is unconditionally stable.

In this paper, the linear, non-parallel wave stability of mixed convection flow along an inclined flat plate is studied for the entire range of inclination angles γ from 0° (horizontal) to 90° (vertical). In the study, the above-mentioned method of ref. [7] is extended to treat the coupling between the momentum and thermal fields in the stability problem. The analysis is based on the quasi-parallel flow model in refs. [3, 9, 10], but a correction is made to account for the effect of the nonparallelism of the disturbance ampli-

tude functions. Owing to the use of a superposition technique along with a modified Thomas transformation [8] for solving the non-homogeneous disturbance equations, the present non-parallel flow model analysis is very efficient and consumes only about 10% more CPU time than the quasi-parallel flow model.

ANALYSIS AND SOLUTION METHOD

As demonstrated in ref. [10] the disturbance equations based on the linear theory for two-dimensional, incompressible flow along an inclined flat plate are

$$\partial^2\tilde{U}/\partial Y\partial t-\partial^2\tilde{V}/\partial X\partial t+U(\partial^2\tilde{U}/\partial Y\partial X-\partial^2\tilde{V}/\partial X^2)+V(\partial^2\tilde{U}/\partial Y^2-\partial^2\tilde{V}/\partial Y\partial X)+\tilde{V}\partial^2U/\partial Y^2-\tilde{U}\partial^2V/\partial Y^2=\nu[(\partial/\partial Y)(\partial^2\tilde{U}/\partial X^2+\partial^2\tilde{U}/\partial Y^2)-(\partial/\partial X)(\partial^2\tilde{V}/\partial X^2+\partial^2\tilde{V}/\partial Y^2)]\pm g\beta\sin\gamma\,\partial\tilde{T}/\partial Y\mp g\beta\cos\gamma\,\partial\tilde{T}/\partial X \quad (1)$$

$$\partial\tilde{T}/\partial t+U\partial\tilde{T}/\partial X+\tilde{U}\partial T/\partial X+V\partial\tilde{T}/\partial Y+\tilde{V}\partial T/\partial Y=(k/\rho c_p)(\partial^2\tilde{T}/\partial X^2+\partial^2\tilde{T}/\partial Y^2) \quad (2)$$

where the tildes denote disturbance quantities and the boundary layer approximation has been applied to the mainflow quantities. The inclination angle γ is measured from the horizontal position. In the present investigation, artificial disturbances are imposed at a certain axial location X_0 from the leading edge of the flat plate and observations are made at an arbitrary downstream location X. The disturbances are assumed to have the form of a wave traveling in the streamwise direction X with its amplitude functions depending on both X and Y. That is

$$\tilde{U}=\partial\tilde{\Psi}/\partial Y,\quad \tilde{V}=-\partial\tilde{\Psi}/\partial X$$

$$\tilde{\Psi}=\tilde{\Phi}(X,Y)\exp\left(\mathrm{i}\int_{X_0}^{X}\tilde{\alpha}\,\mathrm{d}X-\mathrm{i}\tilde{\omega}t\right)$$

$$\tilde{T}=\tilde{S}(X,Y)\exp\left(\mathrm{i}\int_{X_0}^{X}\tilde{\alpha}\,\mathrm{d}X-\mathrm{i}\tilde{\omega}t\right). \quad (3)$$

For the spatial mode of disturbances considered here, the wave number $\tilde{\alpha}=\tilde{\alpha}_r+\mathrm{i}\tilde{\alpha}_i$ is a complex function of X and the wave frequency $\tilde{\omega}$ is regarded as a real constant. It is noted that in parallel and quasi-parallel flow models, the amplitude function of disturbances $\tilde{\Phi}$ and $\tilde{S}$ are assumed to be independent of X and the wave number thus can be uniquely defined. The wave number and the amplitude functions of velocity and temperature based on the quasi-parallel flow model [10] are, respectively, defined as $\tilde{\alpha}_0$, $\tilde{\Phi}_0$ and $\tilde{S}_0$. For the non-parallel flow model, owing to the X-dependence of $\tilde{\alpha}$, $\tilde{\Phi}$ and $\tilde{S}$, corrections on them must be made. The corrected quantities are assumed to have the form

$$\tilde{\alpha}=\tilde{\alpha}_0+\varepsilon\tilde{\alpha}_1,\quad \tilde{\Phi}=\tilde{\Phi}_0+\varepsilon\tilde{\Phi}_1,\quad \tilde{S}=\tilde{S}_0+\varepsilon\tilde{S}_1 \quad (4)$$

where ε is a small positive real number and can be defined as $\varepsilon=\delta/X_c$ such that $\tilde{\alpha}_1$, $\tilde{\Phi}_1$ and $\tilde{S}_1$ have the same order of magnitude as $\tilde{\alpha}_0$, $\tilde{\Phi}_0$ and $\tilde{S}_0$, respectively. For the quasi-parallel flow model, ε is identically zero.

Substituting equations (3) and (4) into equations (1) and (2), and using the following dimensionless quantities

$$\Phi_0=\tilde{\Phi}_0/U_c\delta,\quad \Phi_1=\tilde{\Phi}_1/U_c\delta,\quad S_0=\tilde{S}_0/T_c,$$
$$S_1=\tilde{S}_1/T_c,\quad \alpha_0=\tilde{\alpha}_0\delta,\quad \alpha_1=\tilde{\alpha}_1\delta,\quad \omega=\tilde{\omega}\delta/U_c,$$
$$u=U/U_c,\quad v=(X/\delta)V/U_c,\quad \theta=(T-T_\infty)/T_c,$$
$$\lambda=Re_\delta,\quad \zeta=\pm Gr_\delta/Re_\delta,\quad \Omega=X\,\partial\theta/\partial X+n\theta,$$
$$n=(X/T_c)(\mathrm{d}T_c/\mathrm{d}X),\quad Re_\delta=U_c\delta/\nu,$$
$$Gr_\delta=g\beta|T_c|\delta^3/\nu^2,\quad y=Y/\delta,\quad x=X/X_c. \quad (5)$$

one obtains:

$O(1)$ level

$$L_{11}(\Phi_0)+L_{12}(S_0)=0 \quad (6a)$$

$$L_{21}(\Phi_0)+L_{22}(S_0)=0 \quad (6b)$$

$$\Phi_0(x,0)=\Phi_0'(x,0)=\Phi_0(x,\infty)=\Phi_0'(x,\infty)=0 \quad (6c)$$

$$k_1S_0'(x,0)+k_2S_0(x,0)=S_0(x,\infty)=0; \quad (6d)$$

$O(\varepsilon)$ level

$$L_{11}(\Phi_1)+L_{12}(S_1)=\mathrm{i}\alpha_1M_{11}(\alpha_0,\Phi_0,S_0)+M_{12}(\alpha_0,\alpha_x,\Phi_0,\Phi_x,S_x) \quad (7a)$$

$$L_{21}(\Phi_1)+L_{22}(S_1)=\mathrm{i}\alpha_1M_{21}(\alpha_0,\Phi_0,S_0)+M_{22}(\alpha_0,\alpha_x,S_0,\Phi_x,S_x) \quad (7b)$$

$$\Phi_1(x,0)=\Phi_1'(x,0)=\Phi_1(x,\infty)=\Phi_1'(x,\infty)=0 \quad (7c)$$

$$k_1S_1'(x,0)+k_2S_1(x,0)=S_1(x,\infty)=0 \quad (7d)$$

where

$$L_{11}(\Phi)=\Phi^{\mathrm{iv}}+a_1\Phi'''+a_2\Phi''+a_3\Phi'+a_4\Phi$$
$$L_{12}(S)=a_5S'+a_6S$$
$$L_{21}(\Phi)=b_3\Phi'+b_4\Phi$$
$$L_{22}(S)=S''+b_1S'+b_2S$$
$$M_{11}(\alpha_0,\Phi_0,S_0)=a_7\Phi_0+a_8\Phi_0'+a_9\Phi_0+a_{10}S_0$$
$$M_{12}(\alpha_0,\alpha_x,\Phi_0,\Phi_x,S_x)=a_7\Phi_x''+a_8\Phi_x'+a_9\Phi_x+a_{10}S_x+a_{11}\alpha_x$$
$$M_{21}(\alpha_0,\Phi_0,S_0)=b_5\Phi_0+b_6S_0$$
$$M_{22}(\alpha_0,\alpha_x,S_0,\Phi_x,S_x)=b_5\Phi_x+b_6S_x+b_7\alpha_x \quad (8)$$

and

$$a_1=-v,\quad a_2=-2\alpha_0^2-\mathrm{i}\lambda(\alpha_0u-\omega),\quad a_3=\alpha_0^2v+v''$$
$$a_4=\alpha_0^4+\mathrm{i}\alpha_0\lambda(\alpha_0^2u-\omega\alpha_0+u''),\quad a_5=\zeta\sin\gamma$$
$$a_6=-\mathrm{i}\alpha_0\zeta\cos\gamma,\quad a_7=\lambda u-4\mathrm{i}\alpha_0,\quad a_8=2\mathrm{i}v\alpha_0$$
$$a_9=\lambda(2\omega\alpha_0-3u\alpha_0^2-u'')+4\mathrm{i}\alpha_0^3,\quad a_{10}=\zeta\cos\gamma$$
$$a_{11}=-2\mathrm{i}\Phi_0''+\mathrm{i}v\Phi_0'+(\lambda\omega-3\lambda\alpha_0u+6\mathrm{i}\alpha_0^2)\Phi_0$$

$$b_1 = Pr\, a_1, \quad b_2 = -\alpha_0^2 - i\lambda\, Pr\,(\alpha_0 u - \omega)$$

$$b_3 = -Pr\,\Omega, \quad b_4 = i\alpha_0 \lambda\, Pr\,\theta', \quad b_5 = -Pr\,\lambda\theta'$$

$$b_6 = Pr\,\lambda u - 2i\alpha_0, \quad b_7 = -iS_0 \tag{9}$$

with $\zeta = \pm Gr_\delta/Re_\delta$, $\alpha_x = d\alpha_0/dx$, $\Phi_x = \partial\Phi_0/\partial x$ and $S_x = \partial S_0/\partial x$.

The primes in equations (6)–(9) stand for partial differentiation with respect to y. In the derivation of equations (6)–(9), the higher derivative terms $\partial^2/\partial X^2$, $\partial^3/\partial X^3$ and $\partial^4/\partial X^4$ and the higher level equations of $O(\varepsilon^2)$ and smaller have been neglected. The form of boundary conditions (6d) and (7d) at $y = 0$ will vary according to the appropriate thermal boundary condition. For the case of uniform wall temperature treated in this paper, they are, respectively

$$S_0(x,0) = S_0(x,\infty) = 0 \tag{10a}$$

$$S_1(x,0) = S_1(x,\infty) = 0. \tag{10b}$$

In equation (5), the quantities $\delta(X)$, X_c, $U_c(X)$ and $T_c(X)$ are, respectively, the characteristic boundary layer thickness, characteristic axial length, characteristic streamwise velocity and characteristic temperature. It should be pointed out here that the present analysis is based on a local observation position X. The characteristic quantities δ, X_c, U_c and T_c thus can be treated as constants in the nondimensionalization, equation (5). This point has been clarified well in the past [7]. The quantities $\delta(X)$, $U_c(X)$ and $T_c(X)$ are defined accordingly for individual flow cases and appropriate thermal boundary conditions. The characteristic length X_c, however, is defined such that variations of quantities with respect to x are of the order of unity. That is

$$\partial/\partial x = X_c\,\partial/\partial X = O(1). \tag{11}$$

For the quasi-parallel flow model, the assumption $\partial/\partial X = 0$ leads to $X_c = \infty$ (see equation (11)) and thus $\varepsilon = \delta/X_c = 0$. In the present non-parallel flow model, the value of ε is

$$\varepsilon = \delta/X_c = \delta/X \tag{12}$$

because of the boundary layer approximation ($X_c = X$) and the system of equations (7) is used to account for the effect of variations of α_0, Φ_0 and S_0 in the streamwise direction. Hence, the quantities α_x, Φ_x and S_x must be determined before the system of equations (7) can be solved.

To determine α_x, Φ_x and S_x, the first step is to differentiate equations (6a)–(6c) and (10a) with respect to x. This yields

$$L_{11}(\Phi_x) + L_{12}(S_x) = \alpha_x N_{11}(\alpha_0, \Phi_0, S_0) + N_{12}(\alpha_0, \Phi_0, S_0) \tag{13a}$$

$$L_{21}(\Phi_x) + L_{22}(S_x) = \alpha_x N_{21}(\alpha_0, \Phi_0, S_0) + N_{22}(\alpha_0, \Phi_0, S_0) \tag{13b}$$

$$\Phi_x(x,0) = \Phi_x'(x,0) = \Phi_x(x,\infty) = \Phi_x'(x,\infty) = 0 \tag{13c}$$

$$S_x(x,0) = S_x(x,\infty) = 0 \tag{13d}$$

where

$$N_{11}(\alpha_0, \Phi_0, S_0) = (4\alpha_0 + i\lambda u)\Phi_0'' - 2\alpha_0 v\Phi_0' - (4\alpha_0^3 + i3\lambda\alpha_0^2 u - i2\omega\alpha_0\lambda + i\lambda u'')\Phi_0 - i\zeta_x \cos\gamma\, S_0$$

$$N_{12}(\alpha_0, \Phi_0, S_0) = v_x\Phi_0''' + i\lambda\alpha_0 u_x\Phi_0'' - [\alpha_0^2 v_x + (v'')_x]\Phi_0' - i\alpha_0\lambda[\alpha_0^2 u_x + (u'')_x]\Phi_0 - \zeta_x \sin\gamma\, S_0' - i\alpha_0\zeta_x \cos\gamma\, S_0$$

$$N_{21}(\alpha_0, \Phi_0, S_0) = (2\alpha_0 + i\lambda\, Pr\, u)S_0 - i\lambda\, Pr\,\theta'\Phi_0$$

$$N_{22}(\alpha_0, \Phi_0, S_0) = Pr\, v_x S_0' + i\lambda\, Pr\,\alpha_0 u_x S_0 + Pr\,\Omega_x\Phi_0' - i\alpha_0\lambda\, Pr\,(\theta')_x\Phi_0 \tag{14}$$

with $u_x = \partial u/\partial x$, $(u'')_x = \partial u''/\partial x$, etc. In summary, the stability problem under study is governed by the systems of equations (6), (13) and (7). These equations have the same eigenvalue α_0 which can be found by solving the eigenvalue problem described by the system of equations (6). The values of α_x and α_1 are to be determined such that solutions of the systems of equations (13) and (7) exist.

The formulation of the instability problem, represented by the systems of equations (6), (13) and (7), is performed on a general basis. For individual applications, the mainflow quantities u, v, u'', v'', θ', Ω, u_x, v_x, $(u'')_x$, $(v'')_x$, $(\theta')_x$ and Ω_x are determined from the appropriate mainflow configuration. In the present investigation, wave stability of mixed convection flow along an isothermal inclined flat plate is considered. The corresponding mainflow quantities are given in Appendix A. Once the mainflow quantities are available for given values of ξ, γ and Pr, the system of equations (6) can be solved by a modified Thomas transformation method [8] to yield α_0 for given ω and λ. The result can be expressed in the form

$$\Phi_0(x,y) = \Phi_0''(x,0)\phi_0(x,y) \tag{15a}$$

$$S_0(x,y) = \Phi_0''(x,0)s_0(x,y) \tag{15b}$$

where $\Phi_0''(x,0)$ is an arbitrary function of x and $\phi_0(x,y)$ and $s_0(x,y)$ satisfy

$$L_{11}(\phi_0) + L_{12}(s_0) = 0 \tag{16a}$$

$$L_{21}(\phi_0) + L_{22}(s_0) = 0 \tag{16b}$$

$$\phi_0'(x,0) = \phi_0''(x,0) - 1 = \phi_0(x,\infty) = \phi_0'(x,\infty) = 0 \tag{16c}$$

$$s_0(x,0) = s_0(x,\infty) = 0. \tag{16d}$$

The eigenvalue α_0 is determined to satisfy the boundary condition $\phi_0(x,0) = 0$.

Substituting equations (15) into equations (13) and solving the resulting equations by a superposition technique, as described in Appendix B, one has

$$\Phi_x(x,y) = \Phi_x''(x,0)\phi_0(x,y) + \Phi_0''(x,0)\phi_{x,\mathrm{nh}}(x,y)$$
$$= \Phi_0''(x,0)[e\phi_0(x,y) + \phi_{x,\mathrm{nh}}(x,y)]$$
$$S_x(x,y) = \Phi_0''(x,0)[es_0(x,y) + s_{x,\mathrm{nh}}(x,y)] \quad (17)$$

where $e = \Phi_x''(x,0)/\Phi_0''(x,0)$ is an arbitrary function of x, and the functions $\phi_{x,\mathrm{nh}}$ and $s_{x,\mathrm{nh}}$ are defined, respectively, by

$$\phi_{x,\mathrm{nh}}(x,y) = \alpha_x\phi_{x,a}(x,y) + \phi_{x,b}(x,y)$$
$$s_{x,\mathrm{nh}}(x,y) = \alpha_x s_{x,a}(x,y) + s_{x,b}(x,y) \quad (18)$$

in which $\phi_{x,a}$ and $s_{x,a}$ satisfy

$$L_{11}(\phi_{x,a}) + L_{12}(s_{x,a}) = N_{11}(\alpha_0, \phi_0, s_0)$$
$$L_{21}(\phi_{x,a}) + L_{22}(s_{x,a}) = N_{21}(\alpha_0, \phi_0, s_0)$$
$$\phi_{x,a}'(x,0) = \phi_{x,a}''(x,0) = \phi_{x,a}(x,\infty) = \phi_{x,a}'(x,\infty) = 0$$
$$s_{x,a}(x,0) = s_{x,a}(x,\infty) = 0 \quad (19)$$

and $\phi_{x,b}$ and $s_{x,b}$ satisfy

$$L_{11}(\phi_{x,b}) + L_{12}(s_{x,b}) = N_{12}(\alpha_0, \phi_0, s_0)$$
$$L_{21}(\phi_{x,b}) + L_{22}(s_{x,b}) = N_{22}(\alpha_0, \phi_0, s_0)$$
$$\phi_{x,b}'(x,0) = \phi_{x,b}''(x,0) = \phi_{x,b}(x,\infty) = \phi_{x,b}'(x,\infty) = 0$$
$$s_{x,b}(x,0) = s_{x,b}(x,\infty) = 0. \quad (20)$$

The value of α_x can be uniquely determined by the boundary condition $\Phi_x(x,0) = 0$, which gives

$$\alpha_x = -\phi_{x,b}(x,0)/\phi_{x,a}(x,0) \quad (21)$$

from equations (17) and (18).

Similarly, substitution of equations (15) and (17) into equations (7) leads to

$$\mathrm{i}\alpha_e = \mathrm{i}\alpha_1 + e = -\phi_{1,b}(x,0)/\phi_{1,a}(x,0) \quad (22)$$

where $\phi_{1,a}(x,y)$ and $s_{1,a}(x,y)$ satisfy

$$L_{11}(\phi_{1,a}) + L_{12}(s_{1,a}) = M_{11}(\alpha_0, \phi_0, s_0)$$
$$L_{21}(\phi_{1,a}) + L_{22}(s_{1,a}) = M_{21}(\alpha_0, \phi_0, s_0)$$
$$\phi_{1,a}'(x,0) = \phi_{1,a}''(x,0) = \phi_{1,a}(x,\infty) = \phi_{1,a}'(x,\infty) = 0$$
$$s_{1,a}(x,0) = s_{1,a}(x,\infty) = 0 \quad (23)$$

and $\phi_{1,b}(x,y)$ and $s_{1,b}(x,y)$ satisfy

$$L_{11}(\phi_{1,b}) + L_{12}(s_{1,b}) = M_{12}(\alpha_0, \alpha_x, \phi_0, \phi_{x,\mathrm{nh}}, s_{x,\mathrm{nh}})$$
$$L_{21}(\phi_{1,b}) + L_{22}(s_{1,b}) = M_{22}(\alpha_0, \alpha_x, s_0, \phi_{x,\mathrm{nh}}, s_{x,\mathrm{nh}})$$
$$\phi_{1,b}'(x,0) = \phi_{1,b}''(x,0) = \phi_{1,b}(x,\infty) = \phi_{1,b}'(x,\infty) = 0$$
$$s_{1,b}(x,0) = s_{1,b}(x,\infty) = 0. \quad (24)$$

It should be noted that the value of $\mathrm{i}\alpha_e$ can be uniquely determined by equation (22); however, α_1 depends on the arbitrary function e. Note also that for a flow with the particular characteristics

$$u_x = v_x = (u'')_x = (v'')_x = (\theta')_x = \Omega_x = \zeta_x = 0$$

the non-homogeneous terms N_{12} and N_{22} disappear, see equations (14). This results in $\phi_{x,b} = s_{x,b} = 0$ (equations (20)), and therefore $\alpha_x = 0$ and $\phi_{x,\mathrm{nh}} = s_{x,\mathrm{nh}} = 0$. This in turn gives zero values for α_e, $\phi_{1,\mathrm{nh}}$ and $s_{1,\mathrm{nh}}$. Under this particular situation, the present non-parallel flow model reduces to the quasi-parallel flow model.

DEFINITION OF NEUTRAL STABILITY CURVES

As mentioned earlier, the definition of the growth rate of disturbances depends on the use of a physical disturbance quantity, such as a velocity component, stream function, or intensity. The proper choice of a physical quantity for use in the definition of the growth rate of the disturbance is very important. It should be noted that as the fluctuating velocity components in a turbulent flow, the disturbance velocity components $|\tilde{U}|$ and $|\tilde{V}|$ have the same order of magnitude. In turbulent flows, the turbulent intensity is widely used as an indicator of the strength of turbulence. It is thus reasonable to employ the disturbance intensity as the criterion for the disturbance growth rate. Based on the disturbance intensity, ref. [7] studied the non-parallel wave instability of the Blasius flow. The neutral stability curve obtained for this flow is in excellent agreement with the experimental data of Schubauer and Skramstad [1] and of Ross *et al.* [2]. In the present study of mixed convection flow, the velocity disturbance intensity will dominate the wave instability characteristics because the effect of the temperature disturbance on the instability of laminar flow is expected to be small, especially in the forced convection dominated mixed convection regime. The present study, therefore, employes the velocity disturbance intensity as the criterion.

At an observation location X, the intensity of the disturbance can be evaluated from

$$I = (|\tilde{U}|^2 + |\tilde{V}|^2)^{1/2}/U_e = E\exp\left(-\int_{X_0}^{X} \tilde{\alpha}_i \,\mathrm{d}X\right) \quad (25a)$$

or

$$I(x,y)/E(x_0,y) = \exp\left[-\int_{x_0}^{x} (\alpha_i/\varepsilon - \bar{\beta})\,\mathrm{d}x\right] \quad (25b)$$

where $E(x_0,y)$ is the intensity of the disturbance imposed at x_0, and

$$E = (|\Phi'|^2 + |\varepsilon\,\partial\Phi/\partial x + \mathrm{i}\alpha\Phi|^2)^{1/2} \quad (25c)$$
$$\bar{\beta} = E_x/E. \quad (25d)$$

Since both x_0 and x are arbitrary, for a stable flow to exist the integrand in the exponential power of equation (25b) should maintain a positive value as the disturbance travels along the streamwise direction. Thus

$$\alpha_i - \varepsilon\bar{\beta} \geqslant 0 \quad (26a)$$

or

$$(\alpha_0)_i - \varepsilon[\bar{\beta} - (\alpha_1)_i] \geqslant 0. \quad (26b)$$

Substitution of equations (15), (17) and (22) into equations (25c), (25d) and (26b) yields

$$(\alpha_0)_i - \varepsilon[\beta - (\alpha_e)_i] \geqslant 0 \tag{27a}$$

where

$$\beta = \frac{\phi_0' \cdot \phi_{x,nh}' + (\alpha_0 \cdot \alpha_x)|\phi_0|^2 + |\alpha_0|^2(\phi_0 \cdot \phi_{x,nh})}{|\phi_0'|^2 + |\alpha_0|^2|\phi_0|^2} \tag{27b}$$

and

$$\bar{\beta} = e + \beta. \tag{27c}$$

It is noted that the high order terms $O(\varepsilon)$ have been neglected from equation (27b), and the dot "·" denotes a vector inner product if the complex numbers are regarded as two-dimensional vectors, i.e.

$$\alpha = \alpha_r + i\alpha_i = \alpha_r \mathbf{i} + \alpha_i \mathbf{j}. \tag{28}$$

With the definition of equation (27b), β is a real function of y and has the maximum value that occurs at $y = y_c$, i.e. $\beta_{max} = \beta(y_c)$. As in ref. [7], $e = \Phi_x''(x,0)/\Phi_0''(x,0)$ in equation (27c) is treated as a real function of x. A detailed discussion on this can be found in ref. [7]. The neutral stability curve thus can be defined as the curve that satisfies

$$(\alpha_0)_i - \varepsilon[\beta_{max} - (\alpha_e)_i] = 0. \tag{29}$$

When equation (29) is satisfied, the least stable point (x, y_c) is just neutrally stable, and all of the points at $y \neq y_c$ are stable. The flow in the wall region is expected to be unconditionally stable because at the wall ($y = 0$) the denominator of the function β is identically zero (see equation (27b)) such that the value $\beta(x,0)$ becomes negative infinity.

RESULTS AND DISCUSSION

Numerical results for neutral stability curves and critical Reynolds numbers were obtained for Prandtl numbers of 0.7 and 7. Computations were performed for inclination angles of $\gamma = 0°$ and $5° \leqslant \gamma \leqslant 90°$, where γ is measured from the horizontal position. The buoyancy parameter Gr_x/Re_x^2 ranged from 0 to 1 for assisting flow and from 0 to -0.15 for opposing flow. For given values of ω and λ the stability equations (16), (19), (20), (23) and (24) were solved by a modified Thomas transformation method [8]. The step size of $\Delta y = 0.05$ along with $\eta_\infty = 10$ was found to be adequate for all values of Gr_x/Re_x^2 and γ that were investigated. All computations were done on an IBM 4380 computer.

The neutral stability curves based on the present non-parallel flow model, equation (29), for two representative values of the buoyancy force parameter of $Gr_x/Re_x^2 = 0.1$ and -0.1 are shown in ω vs λ coordinates in Fig. 1 for $Pr = 0.7$ and $\lambda = 0°$, 30° and 90°. The neutral stability curve for the Blasius flow ($Gr_x/Re_x^2 = 0$) is also plotted in Fig. 1 for comparison. Note that for the case of Blasius flow, the results are independent of γ. The region enclosed by the neutral stability curve represents the domain in which the disturbance intensity is amplifying at least at a point inside the boundary layer. The flow is thus regarded as unstable. Along the neutral stability curve the least stable point (x, y_c) is just neutrally stable, and all other points with $y \neq y_c$ are stable. Outside the neutral stability curve, the flow is entirely stable. For $\gamma = 90°$ and 30°, an assisting buoyancy force is seen to stabilize the flow, and this trend is reversed for an opposing buoyancy force. It is also seen from Fig. 1 that a larger value of γ gives a larger buoyancy force effect. This is consistent with physical reasoning. For the case of a horizontal flat plate ($\gamma = 0°$), however, the trend is reversed. This behavior can be explained by noting that there are two terms in the mainflow conservation equation (A2)

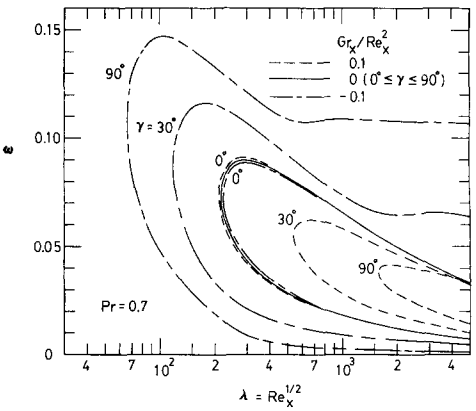

FIG. 1. Neutral stability curves at various angles of inclination for $Gr_x/Re_x^2 = -0.1$, 0 and 0.1.

$$\pm g\beta \sin\gamma (T - T_\infty)$$

and

$$\pm g\beta \cos\gamma \frac{\partial}{\partial X} \int_y^\infty (T - T_\infty)\, dY$$

that stand for the buoyancy force. For convenience, the former is called buoyancy A and the latter buoyancy B. From the transformed equations (A6) and (A16), one sees that buoyancy A is $O(\sin\gamma)$ and buoyancy B is $O(Re_x^{-1/2}\cos\gamma)$ in magnitude. For the cases of $5° \leqslant \gamma \leqslant 90°$, buoyancy B is negligible as compared to buoyancy A because $Re_x^{1/2}$ is very large in the practical situation. The effective buoyancy force thus is proportional to $\sin\gamma$ and has a stabilizing effect on the flow as can be seen from Fig. 1. In the case of a horizontal flat plate ($\gamma = 0°$), buoyancy A disappears and buoyancy B is $O(Re_x^{-1/2})$. In addition, the assisting buoyancy B acts in the direction normal to the forced flow. As a result, it aids in moving the fluid particles away from the plate and thus destabilizes the

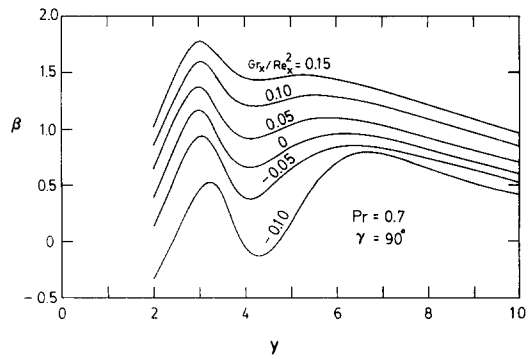

FIG. 2. The function β of the critical points at $\gamma = 90^\circ$ for various values of Gr_x/Re_x^2.

main flow, even though its effect is not that significant. Under the condition of $\gamma \approx \tan^{-1}(Re_x^{-1/2})$ or $0^\circ \leqslant \gamma \leqslant 5^\circ$, both buoyancy A and buoyancy B must be considered. This point will be discussed later. The points having the minimum value of λ on each neutral stability curve are called critical points. The detailed properties at such a point are listed in Table 1 for $Pr = 0.7$ and in Table 2 for $Pr = 7$. Based on these properties, the functions $\beta(y)$ for $Pr = 0.7$ are plotted in Fig. 2 for various values of the buoyancy parameter at $\gamma = 90^\circ$ and in Fig. 3 for representative values of the inclination angle at $\xi = \pm 0.1$. All of the functions β shown in Figs. 2 and 3 possess two humps. The location $y = y_c$ where β reaches its maximum value is the least stable point. It should be noted that the value of $\beta(0)$ is undefined, see equation (27b). Its value is believed to be negative infinity such that the wall region is unconditionally stable due to the existence of a laminar sublayer adjacent to the wall. Figure 2 reveals that the function β increases for an assisting buoyancy force, especially near the inner hump ($y_c \approx 3$) where the least stable point exists. On the other hand, an increasing opposing buoyancy force gives a sharp decrease at the inner hump such that the least stable point jumps from the inner hump to the outer hump ($y_c \approx 6.5$) at a certain buoyancy parameter in the range $-0.10 \leqslant Gr_x/Re_x^2 \leqslant -0.05$. Similar effects can be found in Fig. 3 for $\gamma = 90^\circ$ and 30° because the buoyancy force is proportional to $\sin\gamma$.

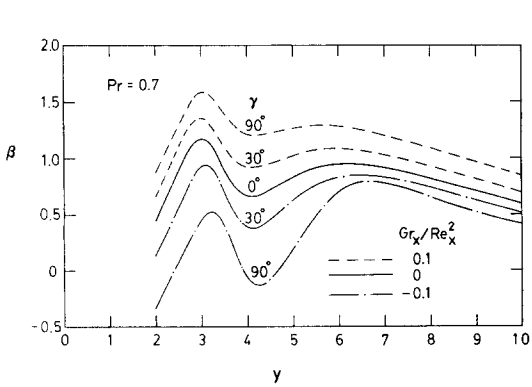

FIG. 3. The function β of the critical points at various angles of inclination for $Gr_x/Re_x^2 = -0.1$, 0 and 0.1.

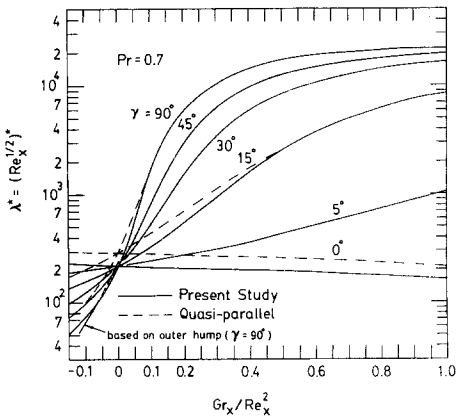

FIG. 4(a). The critical Reynolds number as a function of Gr_x/Re_x^2 for various angles of inclination.

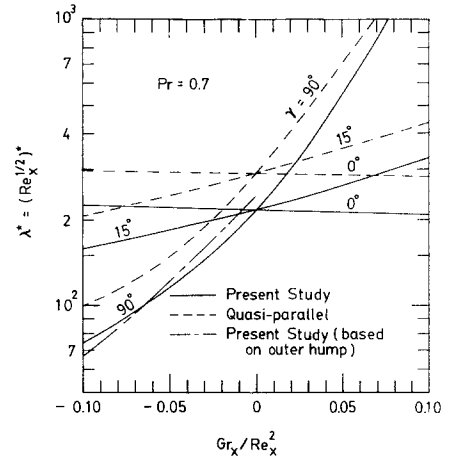

FIG. 4(b). Enlargement of Fig. 4(a) for $-0.1 \leqslant Gr_x/Re_x^2 \leqslant 0.1$.

For the case of a horizontal plate ($\gamma = 0^\circ$) the buoyancy effect on function β is negligible. The trend, however, is reversed. For instance, the values of β_{max} are, respectively, 1.1841, 1.1830 and 1.1787 for $Gr_x/Re_x^{5/2}$ of -0.0005, 0 and 0.0005 or Gr_x/Re_x^2 of -0.111, 0 and 0.106 (see Table 1).

The critical Reynolds number, $\lambda^* = (Re_x^{1/2})^*$, are presented in Fig. 4(a) as a function of the buoyancy parameter Gr_x/Re_x^2 for $Pr = 0.7$ and $\gamma = 90^\circ$, 45°, 30°, 15°, 5° and 0°. For a clearer view, the portion $-0.1 \leqslant Gr_x/Re_x^2 \leqslant 0.1$ is enlarged and shown in Fig. 4(b). The results based on the quasi-parallel flow model [10] are also plotted in Figs. 4(a) and (b). All of the curves from the present non-parallel flow model are seen to pass through the point $Gr_x/Re_x^2 = 0$ and $\lambda^* = 217.4$. This is because the buoyancy effect disappears for all inclination angles $0^\circ \leqslant \gamma \leqslant 90^\circ$ at $Gr_x/Re_x^2 = 0$. The curves for $5^\circ \leqslant \gamma \leqslant 90^\circ$ possess positive slopes which means that an increase in the buoyancy parameter Gr_x/Re_x^2 will stabilize the flow. For the horizontal flat plate ($\gamma = 0^\circ$) the trend is reversed. These behaviors agree with the quasi-parallel flow model. Due to the neglect of the streamwise dependence of wave properties, the quasi-parallel flow

Table 1. Properties of the critical points for $Pr = 0.7$

γ	Gr_x/Re_x^2	λ^*	ω^*	$(\alpha_0)_r^*$	$(\alpha_0)_i^*$	$(\alpha_x)_r^*$	$(\alpha_x)_i^*$	$(\alpha_e)_r^*$	$(\alpha_e)_i^*$	β_{max}^*	y_c
	−0.10†	66	0.10742	0.2186	0.003910	0.1127	−0.04543	−0.1738	0.5410	0.8009	6.679
	−0.05†	122	0.09441	0.2064	0.002598	0.1061	−0.02494	0.0566	0.5060	0.8224	6.315
	0†	241	0.07523	0.1812	0.001743	0.1046	−0.00830	0.2003	0.5150	0.9351	6.088
	−0.15	52	0.11928	0.2340	−0.005562	0.1215	−0.08357	−0.3645	0.4448	0.1574	3.542
	−0.10	74	0.10313	0.2139	0.001683	0.1104	−0.04517	−0.1573	0.5324	0.6568	3.232
	−0.05	116	0.08939	0.1960	0.003460	0.1065	−0.02468	0.0385	0.5458	0.9481	3.083
	0	217	0.07394	0.1764	0.002973	0.1054	−0.00835	0.2021	0.5372	1.1830	2.993
	0.05	550	0.05479	0.1517	0.001394	0.1091	0.00394	0.3123	0.5976	1.3639	2.987
90°	0.10	1583	0.03830	0.1290	0.000520	0.1178	0.00751	0.4126	0.7698	1.5920	3.029
	0.15	3544	0.03026	0.1194	0.000239	0.1257	0.00617	0.5332	0.9246	1.7725	3.021
	0.20	5991	0.02687	0.1175	0.000147	0.1328	0.00461	0.6308	1.0134	1.8951	2.977
	0.40	14246	0.02755	0.1395	0.000069	0.1607	0.00040	0.7707	1.0815	2.0578	2.615
	0.60	18548	0.03314	0.1704	0.000056	0.1889	−0.00151	0.7878	1.0765	2.1155	2.234
	0.80	20881	0.03916	0.1987	0.000051	0.2159	−0.00120	0.7883	1.0826	2.1517	1.948
	1.00	22499	0.04529	0.2252	0.000047	0.2406	−0.00098	0.7822	1.0937	2.1581	1.730
	−0.15	73	0.10343	0.2151	0.001411	0.1096	−0.04924	−0.1783	0.5009	0.6043	3.254
	−0.10	97	0.09442	0.2030	0.003067	0.1068	−0.03277	−0.0372	0.5352	0.8339	3.136
	−0.05	138	0.08469	0.1900	0.003498	0.1055	−0.01962	0.0913	0.5413	1.0238	3.053
	0	217	0.07394	0.1764	0.002973	0.1054	−0.00835	0.2021	0.5372	1.1830	2.993
	0.05	402	0.06086	0.1597	0.001837	0.1074	0.00121	0.2837	0.5671	1.3063	2.973
45°	0.10	853	0.04730	0.1416	0.000931	0.1128	0.00638	0.3464	0.6578	1.4517	2.999
	0.15	1759	0.03711	0.1275	0.000469	0.1189	0.00758	0.4266	0.7903	1.6154	3.027
	0.20	3134	0.03118	0.1201	0.000271	0.1246	0.00675	0.5138	0.9036	1.7919	3.028
	0.40	9923	0.02583	0.1239	0.000093	0.1443	0.00241	0.7209	1.0682	1.9900	2.845
	0.60	14910	0.02814	0.1431	0.000066	0.1642	0.00014	0.7753	1.0813	2.0679	2.565
	0.80	17988	0.03199	0.1646	0.000058	0.1842	−0.00093	0.7890	1.0788	2.1155	2.296
	1.00	19924	0.03634	0.1858	0.000053	0.2036	−0.00140	0.7894	1.0788	2.1397	2.070
	−0.15	96	0.09491	0.2040	0.002963	0.1064	−0.03486	−0.0531	0.5240	0.8075	3.148
	−0.10	120	0.08842	0.1951	0.003435	0.1055	−0.02492	0.0410	0.5379	0.9488	3.087
	−0.05	156	0.08146	0.1859	0.003421	0.1052	−0.01612	0.1264	0.5399	1.0743	3.035
	0	217	0.07394	0.1764	0.002973	0.1054	−0.00835	0.2021	0.5372	1.1830	2.993
	0.05	328	0.06501	0.1650	0.002182	0.1065	−0.00115	0.2623	0.5537	1.2694	2.972
30°	0.10	541	0.05527	0.1525	0.001414	0.1095	0.00390	0.3074	0.5950	1.3604	2.977
	0.15	928	0.04600	0.1398	0.000860	0.1135	0.00678	0.3547	0.6721	1.4702	3.001
	0.20	1556	0.03865	0.1297	0.000527	0.1179	0.00766	0.4109	0.7663	1.5866	3.022
	0.40	5948	0.02698	0.1178	0.000148	0.1329	0.00466	0.6293	1.0121	1.8918	2.974
	0.60	10637	0.02598	0.1260	0.000087	0.1467	0.00199	0.7315	1.0720	2.0003	2.812
	0.80	14208	0.02756	0.1394	0.000069	0.1607	0.00049	0.7709	1.0817	2.0589	2.616
	1.00	16741	0.03010	0.1545	0.000061	0.1749	−0.00048	0.7873	1.0806	2.0980	2.416

Table 1. (*continued*)

γ	Gr_x/Re_x^2	λ^*	ω^*	$(\alpha_0)_r^*$	$(\alpha_0)_i^*$	$(\alpha_x)_r^*$	$(\alpha_x)_i^*$	$(\alpha_c)_r^*$	$(\alpha_c)_i^*$	β_{max}^*	y_c
	−0.15	137	0.08463	0.1903	0.003457	0.1046	−0.02112	0.0815	0.5334	1.0086	3.064
	−0.10	157	0.08123	0.1857	0.003399	0.1047	−0.01651	0.1249	0.5375	1.0715	3.039
	−0.05	183	0.07767	0.1811	0.003227	0.1050	−0.01219	0.1647	0.5386	1.1288	3.014
	0	217	0.07394	0.1764	0.002973	0.1054	−0.00835	0.2021	0.5372	1.1830	2.993
	0.05	263	0.06959	0.1707	0.002587	0.1058	−0.00426	0.2350	0.5452	1.2270	2.980
15°	0.10	329	0.06504	0.1651	0.002178	0.1069	−0.00091	0.2621	0.5537	1.2707	2.968
	0.15	421	0.06012	0.1588	0.001767	0.1082	0.00200	0.2869	0.5709	1.3155	2.967
	0.20	550	0.05504	0.1521	0.001394	0.1099	0.00434	0.3100	0.5978	1.3645	2.976
	0.40	1637	0.03806	0.1289	0.000502	0.1186	0.00786	0.4178	0.7770	1.5987	3.022
	0.60	3714	0.02987	0.1189	0.000230	0.1267	0.00645	0.5437	0.9360	1.7915	3.018
	0.80	6260	0.02678	0.1180	0.000141	0.1340	0.00457	0.6396	1.0199	1.9039	2.965
	1.00	8778	0.02592	0.1216	0.000103	0.1410	−0.00301	0.7004	1.0580	1.9665	2.886
	−0.15	189	0.07691	0.1804	0.003168	0.1045	−0.01247	0.1654	0.5343	1.1317	3.014
	−0.10	197	0.07592	0.1790	0.003104	0.1048	−0.01097	0.1779	0.5367	1.1485	3.007
	−0.05	207	0.07498	0.1777	0.003028	0.1051	−0.00952	0.1898	0.5380	1.1633	2.999
	0	217	0.07394	0.1764	0.002973	0.1054	−0.00835	0.2021	0.5372	1.1830	2.993
	0.05	228	0.07266	0.1745	0.002857	0.1056	−0.00666	0.2134	0.5430	1.1954	2.990
5°	0.10	241	0.07149	0.1730	0.002756	0.1059	−0.00533	0.2239	0.5446	1.2101	2.984
	0.15	256	0.07026	0.1714	0.002647	0.1062	−0.00402	0.2342	0.5466	1.2244	2.979
	0.20	272	0.06899	0.1698	0.002530	0.1065	−0.00277	0.2440	0.5488	1.2380	2.974
	0.40	362	0.06321	0.1624	0.002016	0.1081	0.00174	0.2789	0.5636	1.2930	2.964
	0.60	508	0.05664	0.1539	0.001497	0.1103	0.00520	0.3091	0.5931	1.3536	2.971
	0.80	740	0.04991	0.1450	0.001061	0.1130	0.00743	0.3394	0.6411	1.4258	2.987
	1.00	1087	0.04380	0.1367	0.000739	0.1160	0.00849	0.3741	0.7037	1.5068	3.004
	$Gr_x/Re_x^{5/2}$										
	−0.0040	268	0.06873	0.1714	0.002575	0.1015	−0.01122	0.1961	0.5136	1.2029	3.000
	−0.0020	240	0.07133	0.1739	0.002760	0.1034	−0.00969	0.1989	0.5267	1.1894	2.998
	−0.0015	234	0.07196	0.1745	0.002807	0.1039	−0.00929	0.1997	0.5301	1.1867	2.997
	−0.0010	228	0.07258	0.1750	0.002854	0.1044	−0.00889	0.2004	0.5336	1.1844	2.996
	−0.0005	222	0.07320	0.1756	0.002901	0.1048	−0.00849	0.2011	0.5372	1.1841	2.995
0°	0	217	0.07394	0.1764	0.002973	0.1054	−0.00835	0.2021	0.5372	1.1830	2.993
	0.0005	212	0.07440	0.1766	0.002997	0.1058	−0.00765	0.2026	0.5445	1.1787	2.995
	0.0010	207	0.07498	0.1771	0.003047	0.1062	−0.00722	0.2033	0.5483	1.1776	2.994
	0.0015	202	0.07556	0.1775	0.003098	0.1067	−0.00679	0.2040	0.5522	1.1766	2.993
	0.0020	197	0.07615	0.1780	0.003148	0.1071	−0.00636	0.2047	0.5559	1.1757	2.992
	0.0040	179	0.07837	0.1797	0.003365	0.1089	−0.00455	0.2076	0.5720	1.1757	2.989
	0.0060	164	0.08049	0.1811	0.003604	0.1106	−0.00264	0.2103	0.5888	1.1797	2.985

† Based on the outer hump.

Table 2. Properties of the critical points for $Pr = 7$

γ	Gr_x/Re_x^2	λ^*	ω^*	$(\alpha_0)_r^*$	$(\alpha_0)_i^*$	$(\alpha_x)_r^*$	$(\alpha_x)_i^*$	$(\alpha_c)_r^*$	$(\alpha_c)_i^*$	β_{max}^*	y_c
	−0.15	106	0.09481	0.2132	0.001189	0.1220	−0.04163	−0.1465	0.5176	0.6431	2.997
	−0.10	129	0.08841	0.2013	0.002281	0.1151	−0.02881	−0.0300	0.5281	0.8234	2.994
	−0.05	123	0.08173	0.1894	0.002856	0.1099	−0.01809	0.0842	0.5338	0.9984	2.993
90°	0	217	0.07394	0.1764	0.002973	0.1054	−0.00835	0.2021	0.5372	1.1830	2.993
	0.05	331	0.06283	0.1588	0.002537	0.1024	0.00151	0.3170	0.5531	1.3916	3.028
	0.10	734	0.04554	0.1316	0.001457	0.1038	0.01020	0.4037	0.6228	1.6914	3.139
	0.15	2909	0.02529	0.0969	0.000457	0.1109	0.01139	0.5397	0.9275	2.2568	3.349
	0.20	8762	0.01633	0.0798	0.000180	0.1152	0.00718	0.7813	1.2111	2.7918	3.465
	0.40	50033	0.01020	0.0733	0.000038	0.1217	−0.00054	1.1938	1.3814	3.3062	3.413
	−0.15	181	0.07907	0.1852	0.002875	0.1089	−0.01589	0.1108	0.5312	1.0512	2.994
	−0.10	191	0.07739	0.1822	0.002931	0.1077	−0.01327	0.1412	0.5351	1.0952	2.994
	−0.05	203	0.07565	0.1792	0.002960	0.1065	−0.01071	0.1713	0.5377	1.1384	2.993
	0	217	0.07394	0.1764	0.002973	0.1054	−0.00835	0.2021	0.5372	1.1830	2.993
	0.05	233	0.07176	0.1726	0.002942	0.1043	−0.00566	0.2339	0.5430	1.2278	2.999
15°	0.10	253	0.06954	0.1689	0.002886	0.1034	−0.00319	0.2638	0.5443	1.2737	3.004
	0.15	277	0.06709	0.1650	0.002800	0.1027	−0.00072	0.2938	0.5461	1.3218	3.010
	0.20	310	0.06432	0.1606	0.002665	0.1020	0.00175	0.3227	0.5485	1.3731	3.020
	0.40	658	0.04760	0.1347	0.001607	0.1028	0.01113	0.4154	0.6004	1.6575	3.119
	0.60	3057	0.02481	0.0960	0.004384	0.1113	0.01189	0.5495	0.9364	2.2764	3.354
	0.80	9550	0.01587	0.0789	0.000167	0.1156	0.00698	0.8039	1.2278	2.8272	3.469
	1.00	18942	0.01272	0.0737	0.000093	0.1173	0.00328	0.9877	1.3404	3.1079	3.484
	$Gr_x/Re_x^{5/2}$										
	−0.0040	319	0.06502	0.1642	0.002349	0.1073	−0.00911	0.1837	0.5486	1.2989	3.029
	−0.0020	257	0.07008	0.1711	0.002701	0.1063	−0.00850	0.1934	0.5381	1.2308	3.008
	−0.0015	245	0.07111	0.1725	0.002773	0.1061	−0.00840	0.1958	0.5378	1.2172	3.005
	−0.0010	234	0.07206	0.1738	0.002841	0.1059	−0.00831	0.1981	0.5381	1.2048	3.001
	−0.0005	225	0.07295	0.1749	0.002905	0.1056	−0.00824	0.2004	0.5391	1.1933	2.998
0°	0	217	0.07394	0.1764	0.002973	0.1054	−0.00835	0.2021	0.5372	1.1830	2.993
	0.0005	209	0.07454	0.1770	0.003022	0.1051	−0.00811	0.2048	0.5426	1.1732	2.993
	0.0010	201	0.07526	0.1779	0.003076	0.1049	−0.00805	0.2068	0.5449	1.1643	2.991
	0.0015	195	0.07594	0.1787	0.003127	0.1047	−0.00801	0.2089	0.5475	1.1561	2.989
	0.0020	188	0.07657	0.1795	0.003176	0.1045	−0.00796	0.2109	0.5504	1.1486	2.987
	0.0040	167	0.07872	0.1819	0.003355	0.1036	−0.00780	0.2183	0.5646	1.1247	2.980
	0.0060	150	0.08037	0.1836	0.003511	0.1028	−0.00765	0.2252	0.5816	1.1085	2.976

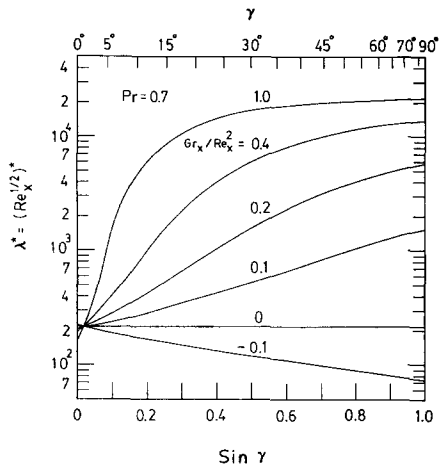

FIG. 5. The critical Reynolds number as a function of $\sin\gamma$ for various values of Gr_x/Re_x^2.

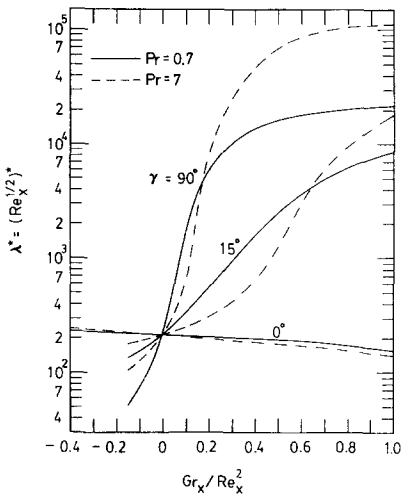

FIG. 6. The effect of Prandtl number on the critical Reynolds number.

model overpredicts the critical Reynolds number by a great amount. For example, for $Gr_x/Re_x^2 = 0$ the quasi-parallel flow model gives $\lambda^* = 290$ which is about 33% higher than the present result of $\lambda^* = 217.4$ and the experimental data of $\lambda^* = 220$ [1, 2]. For an opposing buoyancy force, the overprediction is even larger. Unfortunately, there are no experimental data available to verify the present results for the case of mixed convection flow. When λ is sufficiently large or $\varepsilon = 1/\lambda$ is sufficiently small, the present definition of the neutral stability curve, equation (29), reduces to $(\alpha_0)_i = 0$. Thus, the quasi-parallel flow model is expected to give a good prediction for $\lambda > 3000$ as can be seen from Fig. 4(a).

It is pointed out here that for the vertical plate ($\gamma = 90°$), the critical Reynolds numbers based on the outer hump of function β (see Figs. 2 and 3) are obtained for the case of an opposing buoyancy force. From Fig. 4(b), one can see that for $Gr_x/Re_x^2 < -0.066$, the outer hump overtakes the inner hump and gives a smaller critical Reynolds number. For small inclination angles, the buoyancy effect is not as significant. The curves shown in Fig. 4(a) for $\gamma = 5°$ and 0° thus approximate straight lines with a small positive slope for $\gamma = 5°$ and a small negative slope for $\gamma = 0°$.

Based on the behaviors described above, it is expected that there exists a certain value of γ at which the net effect of buoyancy A and buoyancy B becomes zero and thus a straight line of zero slope exists at that inclination angle. This point can be verified by replotting the critical Reynolds number as a function of $\sin\gamma$ for various values of Gr_x/Re_x^2 as shown in Fig. 5. It is interesting to note from Fig. 5 that smooth curves can be constructed in the entire regime of $0 \leqslant \sin\gamma \leqslant 1$ for each value of Gr_x/Re_x^2 that was investigated. As expected, these curves have a common crossover at $\gamma = 1.05°$ (i.e. $\sin\gamma = 0.0183$) where the net effect of the buoyancy force is zero. As a result, for an increase in the value of Gr_x/Re_x^2 the flow will become more stable when $\gamma > 1.05°$ and less stable when $\gamma < 1.05°$. Figure 5 also reveals that an increase in the inclination angle γ stabilizes the flow for an assisting buoyancy force and destabilizes the flow for an opposing buoyancy force.

The critical Reynolds numbers for $Pr = 0.7$ and 7 and for $\gamma = 90°$, 15° and 0° are brought together in Fig. 6 to examine the effect of Prandtl number. Figure 6 illustrates that for weak buoyancy forces an increase in the Prandtl number destabilizes the flow for an assisting buoyancy force and stabilizes it for an opposing buoyancy force. However, for strong assisting buoyancy forces, a higher Prandtl number gives rise to a higher critical Reynolds number. These trends agree with those from the results of quasi-parallel flow model analysis [3, 11].

CONCLUSION

Linear wave instability of mixed convection flow along inclined flat plates is investigated by employing a non-parallel flow model based on the order-of-magnitude analysis. The resulting non-homogeneous, coupled disturbance equations are solved by a superposition technique along with a modified Thomas transformation method without the use of adjoint eigenfunctions. The solutions reveal that for a given buoyancy parameter $|Gr_x/Re_x^2|$ as the inclination angle γ increases the flow becomes more stable for the assisting flow and less stable for the opposing flow. With an increasing value of Gr_x/Re_x^2, the flow is found to become more stable for $\gamma > 1.05°$ and less stable for $\gamma < 1.05°$ when the plate is almost horizontal. At $\gamma = 1.05°$, the net effect of the buoyancy force on the critical Reynolds number appears to be zero in the range of $-0.15 \leqslant Gr_x/Re_x^2 \leqslant 1$.

Acknowledgement—The present work was supported by grants from National Science Foundation (NSF MEA 83-00785) and the University of Missouri (Weldon Spring—Chen 85–86).

REFERENCES

1. G. B. Schubauer and H. K. Skramstad, Laminar boundary-layer oscillations and transition on a flat plate, *J. Res. Nat. Bur. Stand. (U.S.A.)* **38,** 251–292 (1947).
2. J. A. Ross, F. H. Barnes, J. G. Burns and M. A. S. Ross, The flat plate boundary layer. Part 3. Comparison of theory with experiment, *J. Fluid Mech.* **43,** 819–832 (1970).
3. A. Mucoglu and T. S. Chen, Wave instability of mixed convection flow along a vertical flat plate, *Numer. Heat Transfer* **1,** 267–283 (1978).
4. M. Bouthier, Stabilité linéaire des écoulements presque parallèles. Partie II. La couche limite de Blasius, *J. Méc.* **12,** 75–95 (1973).
5. M. Gaster, On the effects of boundary-layer growth on flow stability, *J. Fluid Mech.* **66,** 465–480 (1974).
6. W. S. Saric and A. H. Nayfeh, Nonparallel stability of boundary-layer flows, *Physics Fluids* **18,** 945–950 (1975).
7. S. L. Lee, T. S. Chen and B. F. Armaly, Nonparallel wave instability analysis of boundary layer flows, *Numer. Heat Transfer* **12,** 349–366 (1987).
8. S. L. Lee, T. S. Chen and B. F. Armaly, New finite difference solution methods for wave instability problems, *Numer. Heat Transfer* **10,** 1–18 (1986).
9. T. S. Chen and A. Mucoglu, Wave instability of mixed convection flow over horizontal flat plate, *Int. J. Heat Mass Transfer* **22,** 185–196 (1979).
10. T. S. Chen and A. Moutsoglou, Wave instability of mixed convection flow on inclined surfaces, *Numer. Heat Transfer* **2,** 497–509 (1979).
11. S. L. Lee, T. S. Chen and B. F. Armaly, Wave instability characteristics for the entire regime of mixed convection flow along vertical flat plates, *Int. J. Heat Mass Transfer* **30,** 1743–1751 (1987).
12. S. L. Lee, T. S. Chen and B. F. Armaly, Mixed convection along isothermal vertical cylinders and needles, *Proc. Eighth Int. Heat Transfer Conf.*, Vol. 3, pp. 1425–1432 (1986).

APPENDIX A

The conservation equations for mixed convection flow along an inclined flat plate are

$$\partial U/\partial X+\partial V/\partial Y=0 \tag{A1}$$

$$U\partial U/\partial X+V\partial U/\partial Y=\pm g\beta\sin\gamma(T-T_\infty)\pm g\beta\cos\gamma\frac{\partial}{\partial X}\int_Y^\infty(T-T_\infty)\,\mathrm{d}Y+\nu\partial^2U/\partial Y^2 \tag{A2}$$

$$U\partial T/\partial X+V\partial T/\partial Y=\alpha\partial^2T/\partial Y^2. \tag{A3}$$

The associated boundary conditions are

$$U(X,0)=U_w(X),\quad V(X,0)=V_w(X),\quad U(X,\infty)=U_\infty$$
$$T(0,Y)=T(X,\infty)=T_\infty$$
$$T(X,0)=T_w(X)\quad\text{if } T_w(X)\text{ is known}$$
$$\partial T(X,0)/\partial Y=-q_w(X)/k\quad\text{if } q_w(X)\text{ is known.} \tag{A4}$$

In writing equations (A1)–(A4), the Boussinesq approximations are employed and the fluid properties are assumed to be constants. The plus and minus signs in front of the first buoyancy force term on the right-hand side of equation (A2) apply, respectively, to upward and downward forced flow, while those in front of the second term to flow above and below the plate.

By introducing the general transformation

$$\psi=\nu Xf(\xi,\eta)/\delta,\quad \eta=Y/\delta,\quad \theta=(T-T_\infty)/T_c,\quad \xi=\xi(X),\quad \delta=\delta(X),\quad T_c=T_c(X) \tag{A5}$$

the governing equations (A1) (A3) become

$$f'''+aff''+bf'^2+A\theta+B[p\eta\theta+(p-e)w-c\,\partial w/\partial\xi]=c(f''\,\partial f/\partial\xi-f'\,\partial f'/\partial\xi)$$
$$\theta''+Praf\theta'+Pref'\theta=Prc(\theta'\,\partial f/\partial\xi-f'\,\partial\theta/\partial\xi)$$
$$w'+\theta=0 \tag{A6}$$

where

$$a=1-p,\quad b=2p-1,\quad c=-m\xi,\quad e=-n$$
$$m=(X/\xi)(\mathrm{d}\xi/\mathrm{d}X),\quad n=(X/T_c)(\mathrm{d}T_c/\mathrm{d}X)$$
$$p=(X/\delta)(\mathrm{d}\delta/\mathrm{d}X),\quad A=\sigma|\widehat{Gr}_x|(\delta/X)^{4+j}\sin\gamma$$
$$B=\sigma|\widehat{Gr}_x|(\delta/X)^{5+j}\cos\gamma$$
$$\widehat{Gr}_x=(g\beta T_cX^3/\nu^2)(\delta/X)^{-j}. \tag{A7}$$

The associated boundary conditions are

$$(p-1)f(\xi,0)+c\,\partial f(\xi,0)/\partial\xi=V_w\delta/\nu$$
$$f'(\xi,0)=U_w\delta^2/\nu X,\quad f'(\xi,\infty)=U_\infty\delta^2/\nu X$$
$$j\theta'(\xi,0)+(1-j)\theta(\xi,0)=1-2j$$
$$\theta(\xi,0)=w(\xi,\infty)=0. \tag{A8}$$

In equations (A7), $\sigma=1$ stands for buoyancy assisting flow and $\sigma=-1$ for buoyancy opposing flow. The index j, the characteristic temperature $T_c(X)$ and the general Grashof number $\widehat{Gr}_x$ are defined such that

$$j=0,\quad T_c=T_w(X)-T_\infty,\quad \widehat{Gr}_x=Gr_x\quad\text{if } T_w(X)\text{ is known}$$
$$j=1,\quad T_c=q_w(X)\delta(X)/k,\quad \widehat{Gr}_x=Gr_x^*\quad\text{if } q_w(X)\text{ is known.} \tag{A9}$$

The system of transformed equations (A6) and boundary conditions (A8) can be easily solved by a method proposed in ref. [12]. Once the solution is obtained, the mainflow quantities which are needed for the analysis of wave instability problems are evaluated from

$$u=f',\quad v=(p-1)f+p\eta f'+c\,\partial f/\partial\xi$$
$$u''=f''',\quad v''=p\eta f'''+(3p-1)f''+c\,\partial f''/\partial\xi$$
$$\Omega=(X/T_c)(\partial T/\partial X)=n\theta-p\eta\theta'-c\,\partial\theta/\partial\xi$$
$$\zeta=\sigma(|\widehat{Gr}_x|/Re_x)(U_\infty/U_c)(\delta/X)^{2+j} \tag{A10}$$

and

$$\begin{aligned}
u_x &= -p\eta f''-c\,\partial f'/\partial\xi\\
(u'')_x &= -p\eta f^{\mathrm{iv}}-c\,\partial f'''/\partial\xi\\
v_x &= -p^2\eta^2f''+(p-2p^2-cp_\xi)\eta f'\\
&\quad -cp_\xi f-2p\eta c\,\partial f'/\partial\xi\\
&\quad +(m-p+1+\xi m_\xi)c\,\partial f/\partial\xi\\
&\quad -c^2\,\partial^2f/\partial\xi^2\\
(v'')_x &= -p^2\eta^2f^{\mathrm{iv}}+(p-4p^2-cp_\xi)\eta f'''\\
&\quad -3cp_\xi f''-2p\eta c\,\partial f'''/\partial\xi\\
&\quad +(m-3p+1+\xi m_\xi)c\,\partial f''/\partial\xi\\
&\quad -c^2\,\partial^2f''/\partial\xi^2\\
(\theta')_x &= -p\eta\theta''-c\,\partial\theta'/\partial\xi\\
\Omega_x &= p^2\eta^2\theta''+(p^2-np+cp_\xi)\eta\theta'\\
&\quad -cn_\xi\theta+2p\eta c\,\partial\theta'/\partial\xi\\
&\quad -(m+n+\xi m_\xi)c\,\partial\theta/\partial\xi+c^2\,\partial^2\theta/\partial\xi^2\\
\zeta_x &= X\,\mathrm{d}\zeta/\mathrm{d}X.
\end{aligned} \tag{A11}$$

In the present investigation, forced convection dominated mixed convection flow along an inclined flat plate is considered under the thermal boundary condition of uniform wall temperature without injection and suction ($U_w=V_w=0$). Therefore, δ, U_c and T_c are conveniently defined, respectively, by

$$\delta = X/Re_x^{1/2}, \quad U_e = U_\infty, \quad T_e = T_w - T_\infty = \text{constant} \tag{A12}$$

such that $n = 0, p = 1/2, j = 0, \widehat{Gr}_x = Gr_x, A = \sigma(|Gr_x|/Re_x^2)\sin\gamma, B = \sigma(|Gr_x|/Re_x^{5/2})\cos\gamma$, and the boundary conditions reduce to

$$f(\xi,0) = f'(\xi,0) = f'(\xi,\infty) - 1 = 0$$
$$\theta(\xi,0) - 1 = \theta(\xi,\infty) = w(\xi,\infty) = 0. \tag{A13}$$

The parameters defined in the stability problem are then

$$\lambda = Re_\delta = Re_x^{1/2}, \quad \varepsilon = \delta/X = \lambda^{-1}$$
$$\zeta = \sigma|Gr_x|/Re_x^2, \quad \zeta_x = \zeta. \tag{A14}$$

The pseudo-similarity variable η defined in the mainflow is identical to y defined in the flow stability problems because the flow stability is analyzed at a local value of X or λ.

For the cases of vertical and inclined flat plates ($5^\circ \leqslant \gamma \leqslant 90^\circ$), ξ is defined by

$$\xi = |Gr_x|/Re_x^2. \tag{A15}$$

This gives

$$A = \sigma\xi\sin\gamma, \quad B = \sigma\xi\, Re_x^{-1/2}\cos\gamma$$
$$\zeta = \sigma\xi, \qquad m = 1. \tag{A16}$$

In practical situations, $Re_x^{1/2}$ is usually large and B assumes essentially a value of zero in the range of $5^\circ \leqslant \gamma \leqslant 90^\circ$.

For the case of a horizontal flat plate ($\gamma = 0^\circ$)

$$\xi = |Gr_x|/Re_x^{5/2}, \quad A = 0, \quad B = \sigma\xi$$
$$\zeta = \sigma\xi\lambda, \qquad m = 1/2. \tag{A17}$$

APPENDIX B

Equations (13) and (7) have the common form

$$L_{11}(\Phi) + L_{12}(S) = \Gamma F_{11} + F_{12}$$
$$L_{21}(\Phi) + L_{22}(S) = \Gamma F_{21} + F_{22}$$
$$\Phi(0) = \Phi'(0) = \Phi(\infty) = \Phi'(\infty) = 0$$
$$S(0) = S(\infty) = 0 \tag{B1}$$

where the linear operators L_{11}, L_{12}, L_{21} and L_{22} are defined in equations (8) and (9). They are known after the eigenvalue α_0 is determined by solving the eigenvalue problem described by the system of equations (6) or (16). The non-homogeneous terms F_{11}, F_{12}, F_{21} and F_{22} are all known functions of y. The value of Γ is to be determined such that solution of the system of equations (B1) exists. Since L_{ij} are linear operators, the solution can be superposed by

$$\Phi = \Phi''(0)\phi_a + \Gamma\Phi_b + \Phi_c$$
$$S = \Phi''(0)s_a + \Gamma S_b + S_c \tag{B2}$$

where ϕ_a, s_a, Φ_b, S_b and Φ_c, S_c are, respectively, defined by the system of equations

$$L_{11}(\phi_a) + L_{12}(s_a) = 0$$
$$L_{21}(\phi_a) + L_{22}(s_a) = 0$$
$$\phi_a'(0) = \phi_a''(0) - 1 = \phi_a(\infty) = \phi_a'(\infty) = 0$$
$$s_a(0) = s_a(\infty) = 0 \tag{B3}$$

$$L_{11}(\Phi_b) + L_{12}(S_b) = F_{11}$$
$$L_{21}(\Phi_b) + L_{22}(S_b) = F_{21}$$
$$\Phi_b'(0) = \Phi_b''(0) = \Phi_b(\infty) = \Phi_b'(\infty) = 0$$
$$S_b(0) = S_b(\infty) = 0 \tag{B4}$$

and

$$L_{11}(\Phi_c) + L_{12}(S_c) = F_{12}$$
$$L_{21}(\Phi_c) + L_{22}(S_c) = F_{22}$$
$$\Phi_c'(0) = \Phi_c''(0) = \Phi_c(\infty) = \Phi_c'(\infty) = 0$$
$$S_c(0) = S_c(\infty) = 0. \tag{B5}$$

It should be noted that the solution to the system of equations (B3) is identical to that of the system of equations (16) because the same eigenvalue α_0 obtained from system (16) has been imposed on system (B3). It should also be noted that the present analysis is performed at a local value of X. Therefore, $\phi_a(y) = \phi_0(x,y)$, $\phi_a(0) = \phi_0(x,0) = 0$ and $s_a(y) = s_0(x,y)$. With this, the boundary condition $\Phi(0) = 0$ gives

$$\Phi(0) = \Phi''(0)\phi_a(0) + \Gamma\Phi_b(0) + \Phi_c(0) = 0$$

or

$$\Gamma = -\Phi_c(0)/\Phi_b(0). \tag{B6}$$

The solution of the system of equations (B1) thus has the form

$$\Phi(y) = \Phi''(0)\phi_0(y) + \Phi_{nh}(y)$$
$$S(y) = \Phi''(0)s_0(y) + S_{nh}(y) \tag{B7}$$

where

$$\Phi_{nh}(y) = \Gamma\Phi_b(y) + \Phi_c(y)$$
$$S_{nh}(y) = \Gamma S_b(y) + S_c(y). \tag{B8}$$

This superpositions technique can be verified by multiplying equations (B3), (B4) and (B5), respectively, by $\Phi''(0)$, Γ and unity, and then applying equations (B2). A proof of this approach can be found in ref. [7] for the case of Blasius flow.

INSTABILITE D'ONDE NON PARALLELE POUR LA CONVECTION MIXTE SUR DES PLANS INCLINES

Résumé—Une analyse d'écoulement non parallèle est conduite pour étudier l'instabilité linéaire d'onde dans le cas de la convection mixte sur une plaque plane isotherme inclinée. Les équations couplées, non homogènes pour les perturbations de quantité de mouvement et de température sont résolues par une technique de superposition associée à une méthode de transformation de Thomas modifiée. Les nombres de Reynolds critiques sont présentés pour des angles d'inclinaison $0^\circ \leqslant \gamma \leqslant 90^\circ$ (où γ est repéré par rapport à l'horizontale), pour le paramètre de flottement $-0{,}15 \leqslant Gr_x/Re_x^2 \leqslant 1$ et pour des nombres de Prandtl égaux à 0,7 et 7. On trouve que l'effet de la force d'Archimède sur le nombre de Reynolds critique est essentiellement nul à $\gamma = 1{,}05^\circ$, lorsque la plaque est presque horizontale. Pour $\gamma > 1{,}05^\circ$, un accroissement de Gr_x/Re_x^2 stabilise l'écoulement. Ce comportement est renversé lorsque $\gamma < 1{,}05^\circ$.

DIE NICHT-PARALLELE WELLEN-INSTABILITÄT BEI MISCH-KONVEKTION AN GENEIGTEN EBENEN PLATTEN

Zusammenfassung—Die nicht-parallele lineare Wellen-Instabilität bei Misch-Konvektion an einer isothermen geneigten ebenen Platte wird mittels einer Größenordnungs-Abschätzung untersucht. Diese Abschätzung macht die bisherige Beschränkung auf eine schwache Abhängigkeit von Veränderungen der Störungsintensität in Strömungsrichtung überflüssig. Es ergeben sich nicht-homogene, gekoppelte Gleichungen für die Störungen von Impulstransport und Temperatur. Diese werden mittels einer Überlagerungs-Technik und unter Verwendung einer modifizierten Thomas-Transformation gelöst. Es werden kritische Reynolds-Zahlen für die folgenden Parameter-Bereiche vorgestellt: Neigungswinkel bezüglich der Waagerechten $0° \leqslant \gamma \leqslant 90°$, Auftriebsparameter $-0{,}15 \leqslant Gr_x/Re_x^2 \leqslant 1$, Prandtl-Zahlen 0,7 und 7. Es zeigt sich, daß bei fast waagerechter Platte ($\gamma = 1{,}05°$) der Netto-Effekt der Auftriebskraft auf die kritische Reynolds-Zahl verschwindend klein ist. Für $\gamma > 1{,}05°$ wird die Strömung durch ein Anwachsen von Gr_x/Re_x^2 stabilisiert—das Umgekehrte gilt für $\gamma < 1{,}05°$.

ВОЛНОВАЯ НЕУСТОЙЧИВОСТЬ СМЕШАННОКОНВЕКТИВНОГО ТЕЧЕНИЯ НА НАКЛОННЫХ ПЛОСКИХ ПЛАСТИНАХ

Аннотация—Анализ непараллельных течений методом оценки порядка величин используется для изучения линейной волновой устойчивости смешанноконвективного течения вдоль изотермической наклонной плоской пластины. Данный подход снимает ранее существовавшее ограничение о слабой зависимости величин возмущения вдоль потока. Полученные в результате неоднородные связанные уравнения для возмущений импульса и температуры решаются совместно методом подстановки и модифицированным методом преобразования Томаса. Критические числа Рейнольдса представлены для углов наклона $0° \leqslant \gamma \leqslant 90°$ (причем γ отсчитывается от горизонтали), в диапазоне параметра плавучести $-0.15 \leqslant Gr_x/Re_x^2$ для чисел Прандтля 0.7 и 7. Найдено, что результирующее влияние силы плавучести на критическое число Рейнольдса равно нулю при $\gamma = 1.05°$, когда пластина почти горизонтальна. Для $\gamma > 1.05°$ увеличение значения Gr_x/Re_x^2 стабилизирует течение, а для $\gamma < 1.05°$ наблюдается обратный эффект.